Received: 12 July 2019 | Revised: 5 February 2020 | Accepted: 26 April 2020

DOI: 10.1002/rnc.5038

RESEARCH ARTICLE

WILEY

Observer-based synthesis of linear parameter-varying mixed sensitivity controllers

Julian Theis[1] | **Harald Pfifer**[2]

[1]Institute of Aircraft Systems Engineering, Hamburg University of Technology, Hamburg, Germany

[2]Department of Mechanical, Materials and Manufacturing Engineering, University of Nottingham, Nottingham, United Kingdom

Correspondence
Julian Theis, Institute of Aircraft Systems Engineering, Hamburg University of Technology, Nesspriel 5, 21129 Hamburg, Germany.
Email: julian.theis@tuhh.de

Summary

This article presents a computationally efficient way of synthesizing linear parameter-varying (LPV) controllers. It reviews the possibility of a separate observer and state feedback synthesis with guaranteed performance and shows that a standard mixed sensitivity problem can be solved in this way. The resultant output feedback controller consists of an LPV observer, augmented with dynamic filters to incorporate integral control and roll-off properties, and an LPV state feedback gain. It is thus highly structured, which is beneficial for implementation. Moreover, it does not depend on scheduling parameter rates regardless of whether parameter-dependent Lyapunov matrices are used during synthesis. A representative control design for active flutter suppression on an aeroelastic unmanned aircraft demonstrates the benefits of the proposed method in comparison with state-of-the-art LPV output feedback synthesis.

KEYWORDS

control synthesis algorithm, coprime factorization, flutter suppression, linear parameter-varying control, observer

1 | INTRODUCTION

Linear parameter-varying (LPV) control is a powerful tool for designing self-scheduled control systems. A large body of literature[1-5] and computational tools[6-9] are available. Performance is usually specified in terms of the induced $\mathcal{L}_2$-norm, providing a natural extension of the widely popular $\mathcal{H}_\infty$-control framework.[10] Thus, various control objectives can be specified in a classical mixed sensitivity setting, which makes controller tuning easy. Depending on how exactly the model depends on the scheduling parameter, several approaches exist that formulate the controller synthesis as a semidefinite program (SDP). A widely used approach is to solve the SDP over a gridded parameter space, see Wu et al.[2] This approach is suitable for models with arbitrary parameter dependence, for example, when model data are represented by lookup tables. Such systems include aeroelastic aircraft, the application example in Section 4. Hence, this article focuses on the grid-based approach. When the parameter dependence is affine, polynomial, or rational, the additional structure can be exploited in more efficient computational algorithms.[9,11-15]

LPV controller synthesis, in general, has three major issues: (a) The respective SDP scales badly with the number of state variables and scheduling parameters. (b) The resulting controller is a full-order dynamic controller without

Abbreviations: LPV, linear parameter-varying; LTI, linear time invariant; LMI, linear matrix inequality; SDP, semidefinite program.

any exploitable structure. (c) The controller depends explicitly on the derivative of the scheduling parameters. These parameter variation rates are often difficult to measure, and consequently the rate dependence of the controller is simply omitted in many application examples in the literature. This issue of "practical implementability"[16] has also been addressed through specific synthesis formulations. For instance, Apkarian and Adams[16] offer the possibility to avoid scheduling rate dependence by restricting the Lyapunov matrices in the SDP to a particular structure, which introduces additional conservatism. Sato[17] showed that an outer optimization loop can be formulated such that Lyapunov matrices with a suitable structure are obtained at the expense of increased synthesis complexity.

The main contribution of this article is an observer-based LPV synthesis procedure that alleviates most of the issues of the conventional output feedback synthesis. The article builds on the idea of separate observer and state feedback syntheses introduced by Prempain and Postlethwaite[15,18] as well as Saupe and Pfifer.[19] Contrary to their work, the presented approach retains the mixed sensitivity formulation with its apparent appeal of directly specifying closed-loop performance. That is, a standard mixed sensitivity problem is formulated, but the controller is obtained through an observer synthesis step and a subsequent state feedback synthesis step. It is shown in Section 3 that this procedure guarantees closed-loop performance in terms of the original mixed sensitivity problem. This guarantee is established by means of a specific input weight in the mixed sensitivity formulation. With this input weight, the controller synthesis directly acknowledges the presence of an observer in the loop. The way this input weight is introduced resembles the coprime factorization approach to the parameterization of all stabilizing controllers[20,21] and Kwakernaak's method[22,23] of including pole placement in $\mathcal{H}_\infty$-controller design.

The advantages of the proposed method are as follows. Splitting the synthesis into two separate steps replaces the SDP of the output feedback synthesis with two smaller SDPs, one for the observer and one for the state feedback. As SDPs scale badly with the number of decision variables, solving the two smaller SDPs is much faster than solving the larger original problem. The separate synthesis further leads to a highly structured controller. This structure can be exploited, for example, to facilitate simple antiwindup compensation, see the recent article by the authors.[24] Finally, parameter-dependent Lyapunov matrices can be used for synthesis without leading to dependence on the derivative of the scheduling parameters. This is an immediate consequence of the observer-based structure. While the restriction to an observer-based structure is a source of conservatism, it is shown in the application example in Section 4 that the benefit of using parameter-dependent Lyapunov matrices can outweigh this conservatism.

2 | PRELIMINARIES

LPV systems are a class of dynamic systems whose state space representations depend continuously on a time-varying scheduling parameter vector $\rho : \mathbb{R} \mapsto \mathcal{P}$, where $\mathcal{P} \subset \mathbb{R}^{n_\rho}$ is a compact set of allowable parameters. In addition, the parameter rates $\dot{\rho} : \mathbb{R} \mapsto \mathcal{Q}$ are restricted to lie in a polyhedron $\mathcal{Q} = \{\dot{\rho} \in \mathbb{R}^{n_\rho} | |\dot{\rho}_i| \leq \nu_i,\ i = 1, \dots, n_\rho\}$. Hence, the set of all admissible parameter trajectories is $\mathcal{T} = \{\rho(t) | \rho(t) \in \mathcal{P} \wedge \dot{\rho}(t) \in \mathcal{Q} \quad \forall t \in \mathbb{R}\}$. A state space representation of an LPV system $\mathbf{P}$ is

$$\left[\begin{array}{c} \dot{x}(t) \\ \hline y(t) \end{array}\right] = \left[\begin{array}{c|c} A(\rho(t)) & B(\rho(t)) \\ \hline C(\rho(t)) & D(\rho(t)) \end{array}\right] \left[\begin{array}{c} x(t) \\ \hline u(t) \end{array}\right] \tag{1}$$

where $A : \mathcal{P} \mapsto \mathbb{R}^{n_x \times n_x}$, $B : \mathcal{P} \mapsto \mathbb{R}^{n_x \times n_u}$, $C : \mathcal{P} \mapsto \mathbb{R}^{n_y \times n_x}$, and $D : \mathcal{P} \mapsto \mathbb{R}^{n_y \times n_u}$ are continuous matrix functions. The dependence on parameters and time is from now on occasionally dropped to shorten notation. An input-output perspective proves useful throughout this article and consequently the notation $y = \mathbf{P}\,u$ is used to denote the input-output map established by the state space equations (1) for $x(0) = 0$. Note that the input-output map is independent of state space coordinate transformations.

The performance of an LPV system can be specified in terms of its induced $\mathcal{L}_2$-norm

$$\|\mathbf{P}\| = \sup_{u \in \mathcal{L}_2 \setminus \{0\},\ \rho \in \mathcal{T},\ x(0)=0} \frac{\|y\|_2}{\|u\|_2}\,. \tag{2}$$

Wu et al[2] introduced a generalization of the bounded real lemma that provides an upper bound on $\|\mathbf{P}\|$. The sufficient condition uses a quadratic storage function that is defined using a symmetric positive definite Lyapunov matrix

$P : \mathcal{P} \to \mathbb{R}^{n_x \times n_x}$, which is a continuously differentiable function of the parameter ρ. Positive definiteness of P is denoted $P > 0$, while negative definiteness is denoted $P < 0$. In order to shorten notation, a differential operator $\partial P : \mathcal{P} \times \mathcal{Q} \to \mathbb{R}^{n_x \times n_x}$ is used. It is defined[25] as

$$\partial P(p, q) := \sum_{i=1}^{n_\rho} \frac{\partial P(p)}{\partial p_i} q_i. \tag{3}$$

The next theorem states the condition to bound the $\mathcal{L}_2$-gain of an LPV system.

Theorem 1 (Wu et al[2]). *An LPV system* $\mathbf{P}$ *with state space representation (1) is exponentially stable and* $\|\mathbf{P}\| < \gamma$ *if there exists a continuously differentiable symmetric matrix function* $P : \mathcal{P} \to \mathbb{R}^{n_x \times n_x}$, *such that* $\forall (p, q) \in \mathcal{P} \times \mathcal{Q}$

$$P(p) > 0 \tag{4a}$$

$$\begin{bmatrix} P(p)A(p) + A^T(p)P(p) + \partial P(p, q) & P(p)B(p) \\ B^T(p)P(p) & -I \end{bmatrix} + \frac{1}{\gamma^2} \begin{bmatrix} C^T(p) \\ D^T(p) \end{bmatrix} \begin{bmatrix} C(p) & D(p) \end{bmatrix} < 0. \tag{4b}$$

Proof. The proof resembles the proof of the bounded-real lemma and is detailed in the thesis of Wu.[26] ∎

Theorem 1 leads to conditions that involve the parameter values and rates at all points along any admissible parameter trajectory in $\mathcal{T}$. The parametric description $(p, q) \in \mathcal{P} \times \mathcal{Q}$ emphasizes that such conditions depend only on the sets $\mathcal{P}$ and $\mathcal{Q}$, which can often be approximated by finite dimensional sets such that numerical methods can be applied.

2.1 | Induced $\mathcal{L}_2$-norm controller synthesis

Theorem 1 also forms the basis of induced $\mathcal{L}_2$-norm output feedback controller synthesis as introduced by Wu et al.[2] Consider an open-loop LPV system $\mathbf{G}$ with state space representation

$$\left[\begin{array}{c} \dot{x} \\ \hline z_1 \\ z_2 \\ e \end{array}\right] = \left[\begin{array}{c|ccc} A(\rho) & B_{11}(\rho) & B_{12}(\rho) & B_2(\rho) \\ \hline C_{11}(\rho) & D_{1111}(\rho) & D_{1112}(\rho) & 0 \\ C_{12}(\rho) & D_{1121}(\rho) & D_{1122}(\rho) & I \\ C_2(\rho) & 0 & I & 0 \end{array}\right] \left[\begin{array}{c} x \\ \hline w_1 \\ w_2 \\ u \end{array}\right] \tag{5}$$

and an LPV output feedback controller $\mathbf{K}$ with state space representation

$$\left[\begin{array}{c} \dot{\xi} \\ \hline u \end{array}\right] = \left[\begin{array}{c|c} A_K(\rho, \dot{\rho}) & B_K(\rho) \\ \hline C_K(\rho) & D_K(\rho) \end{array}\right] \left[\begin{array}{c} \xi \\ \hline e \end{array}\right]. \tag{6}$$

The signal e represents a measured error provided to the controller, u is the control variable, and the input-output map from $\begin{bmatrix} w_1 \\ w_2 \end{bmatrix}$ to $\begin{bmatrix} z_1 \\ z_2 \end{bmatrix}$ specifies performance requirements. The special structure of the plant (5) is not restrictive and can, under mild conditions, be achieved through loop-shifting and scalings.[26,27] The objective of the synthesis is to obtain a controller that minimizes the induced $\mathcal{L}_2$-norm of the closed-loop interconnection obtained by connecting the open-loop generalized plant (5) with the controller (6). This connection is given by the lower linear fractional transformation $\mathcal{F}(\mathbf{G}, \mathbf{K})$ such that the synthesis objective can be formulated as $\min_{\mathbf{K}} \|\mathcal{F}(\mathbf{G}, \mathbf{K})\|$. The solution to the induced $\mathcal{L}_2$-norm controller synthesis problem is stated in the next theorem.

Theorem 2 (dynamic output feedback synthesis[26,28]). *Let* $\mathcal{P}$ *and* $\mathcal{Q}$ *be given compact sets and* $\mathbf{G}$ *an LPV system (5). There exists a dynamic output feedback controller* $\mathbf{K}$ *as in Equation (6) such that* $\|\mathcal{F}(\mathbf{G}, \mathbf{K})\| \leq \gamma$ *if there exist continuously*

differentiable, symmetric matrix functions $X : \mathcal{P} \to \mathbb{R}^{n_x \times n_x}$ *and* $Y : \mathcal{P} \to \mathbb{R}^{n_x \times n_x}$ *such that* $\forall (p, q) \in \mathcal{P} \times \mathcal{Q}$

$$\gamma^2 I - \begin{bmatrix} D_{1111}(p) & D_{1112}(p) \\ D_{1121}(p) & D_{1122}(p) \end{bmatrix}^T \begin{bmatrix} D_{1111}(p) & D_{1112}(p) \\ D_{1121}(p) & D_{1122}(p) \end{bmatrix} > 0 \tag{7a}$$

$$\begin{bmatrix} X(p) & I \\ I & Y(p) \end{bmatrix} > 0 \tag{7b}$$

$$\begin{bmatrix} Y(p)\hat{A}^T(p) + \hat{A}(p)Y(p) - \partial Y(p,q) - \gamma B_2(p)B_2^T(p) & Y(p)C_{11}^T(p) & \hat{B}(p) \\ C_{11}(p)Y(p) & -\gamma I & D_{111\bullet}(p) \\ \hat{B}^T(p) & D_{111\bullet}^T(p) & -\gamma I \end{bmatrix} < 0 \tag{7c}$$

$$\begin{bmatrix} \tilde{A}^T(p)X(p) + X(p)\tilde{A}(p) + \partial X(p,q) - C_2^T(p)C_2(p) & X(p)B_{11}(p) & \tilde{C}^T(p) \\ B_{11}^T(p)X(p) & -\gamma I & D_{11\bullet 1}^T(p) \\ \tilde{C}(p) & D_{11\bullet 1}(p) & -\gamma I \end{bmatrix} < 0 \tag{7d}$$

where $\begin{bmatrix} D_{111\bullet}(p) \\ D_{112\bullet}(p) \end{bmatrix} := \begin{bmatrix} D_{1111}(p) & D_{1112}(p) \\ D_{1121}(p) & D_{1122}(p) \end{bmatrix} =: \begin{bmatrix} D_{11\bullet 1}(p) & D_{11\bullet 2}(p) \end{bmatrix}$, $\hat{A}(p) := A(p) - B_2(p)C_{12}(p)$,

$\hat{B}(p) := \begin{bmatrix} B_{11}(p) & B_{12}(p) \end{bmatrix} - B_2(p)\, D_{112\bullet}(p)$, *and* $\tilde{A}(p) := A(p) - B_{12}(p)C_2(p)$, $\tilde{C}(p) := \begin{bmatrix} C_{11}(p) \\ C_{12}(p) \end{bmatrix} - D_{11\bullet 2}(p)\, C_2(p)$.

Proof. The proof is provided in the thesis of Wu.[26] It uses a matrix elimination argument similar to that used by Gahinet and Apkarian[29] in the LMI approach to H_∞-controller synthesis for linear time invariant (LTI) systems. With this, it is possible to construct a matrix $P(p) > 0$ from $X(p)$ and $Y(p)$, which shows that the closed loop satisfies the LMI condition (4) in Theorem 1. An LPV output feedback controller (6) can be explicitly constructed from the open-loop plant matrices and the feasible values of $X(p)$, $Y(p)$, and γ as shown by Wu[26] and Lee.[30] ∎

The closed-loop performance (upper bound) in Theorem 2 can be optimized as a semidefinite program that minimizes γ subject to the LMI constraints (7). The implementation of Theorem 2 as an SDP involves some numerical challenges. The LMI constraints in Theorem 2 are infinite dimensional. Thus, $\mathcal{P}$ and $\mathcal{Q}$ are typically approximated with grids of parameter values to obtain a finite number of LMIs. The number of grid points required for such an approximating can easily become prohibitively large even for a moderate number of scheduling parameters (more than three). In addition, the main decision variables are the functions $X(p)$ and $Y(p)$, which must be restricted to a finite dimensional subspace. A common practice is to restrict $X(p)$ and $Y(p)$ to be linear combinations of prespecified basis functions. However, each additional basis function increases the number of decision variables in the semidefinite program. Finally, note that the resulting output feedback controller, in general, explicitly depends on the parameter variation rate $\dot{\rho}$, even though the plant model only depends on ρ. This rate dependence is a technical consequence of the application of the bounded real lemma with a parameter-dependent storage function and complicates implementation.

In the state feedback case, that is, when $e = x$, the synthesis problem simplifies to the following theorem.

Theorem 3 (static state feedback synthesis[26]). *Let* $\mathcal{P}$ *be a given compact set and* $\mathbf{G}$ *an LPV system (5), but with measurable output* $e = x$. *There exists a static state feedback law* $\mathbf{F} : u = F(\rho)x$ *such that* $\|\mathcal{F}(\mathbf{G}, \mathbf{F})\| \leq \gamma$ *if there exists a continuously differentiable, symmetric matrix function* $Y : \mathcal{P} \to \mathbb{R}^{n_x \times n_x}$ *such that* $\forall (p, q) \in \mathcal{P} \times \mathcal{Q}$

$$\gamma^2 I - \begin{bmatrix} D_{1111}(p) & D_{1112}(p) \\ D_{1121}(p) & D_{1122}(p) \end{bmatrix}^T \begin{bmatrix} D_{1111}(p) & D_{1112}(p) \\ D_{1121}(p) & D_{1122}(p) \end{bmatrix} > 0 \tag{8a}$$

$$Y(p) > 0 \tag{8b}$$

$$\begin{bmatrix} Y(p)\hat{A}^T(p) + \hat{A}(p)Y(p) - \partial Y(p,q) - \gamma B_2(p)B_2^T(p) & Y(p)C_{11}^T(p) & \hat{B}(p) \\ C_{11}(p)Y(p) & -\gamma I & D_{111\bullet}(p) \\ \hat{B}^T(p) & D_{111\bullet}^T(p) & -\gamma I \end{bmatrix} < 0 \tag{8c}$$

where $\begin{bmatrix} D_{111\bullet}(p) \\ D_{112\bullet}(p) \end{bmatrix} := \begin{bmatrix} D_{1111}(p) & D_{1112}(p) \\ D_{1121}(p) & D_{1122}(p) \end{bmatrix}$, $\hat{A}(p) := A(p) - B_2(p)C_{12}(p)$, $\hat{B}(p) := \begin{bmatrix} B_{11}(p) & B_{12}(p) \end{bmatrix} - B_2(p)\, D_{112\bullet}(p)$.

The state feedback gain can be calculated from the open-loop plant matrices and the feasible values of $Y(\rho)$ *and* γ *as*

$$F(\rho) = -(B_2^T + D_{112\bullet}\,\hat{B}^T\,\gamma^{-2} - D_{112\bullet}\,D_{111\bullet}^T\,\gamma^{-2}(D_{111\bullet}\,D_{111\bullet}^T\,\gamma^{-2} - I)^{-1}\,(C_{11}\,Y\,\gamma^{-1} + D_{111\bullet}\,\hat{B}^T\,\gamma^{-2}))\,\gamma\,Y^{-1} - C_{12}. \tag{9}$$

Proof. The proof is provided in the thesis of Wu.[26] ∎

Note that $D_{112\bullet} = 0$ significantly simplifies the expression (9) to $F(\rho) = -(\gamma\, B_2^T Y^{-1} + C_{12})$. In contrast to the output feedback controller, the state feedback gain does not depend on the parameter variation rate $\dot{\rho}$. Furthermore, the SDP is significantly smaller.

2.2 | Coprime factorization

Throughout the article, the notion of a contractive left coprime factorization[15,18,28] plays a central role. A left coprime factorization $\mathbf{P} = \mathbf{M}^{-1}\,\mathbf{N}$ provides a kernel representation of all stable input-output pairs of a system $\mathbf{P}$.[20,21,28] To see this, consider a system $y = \mathbf{P}\,u = \mathbf{M}^{-1}\,\mathbf{N}\,u$. Then, all possible inputs u and outputs y of said system satisfy $\mathbf{M}\,y - \mathbf{N}\,u = 0$. Hence, the set of all input-output pairs is characterized by the null space of $[\mathbf{M}\ \ -\mathbf{N}]$. A *contractive* coprime factorization further has the property $\|[\mathbf{M}\ \ \mathbf{N}]\| \leq 1$. It is defined in the following theorem.

Theorem 4. *Let* $\mathbf{P}$ *be an LPV system with state space representation (1). There exists a contractive left coprime factorization* $\mathbf{P} = \mathbf{M}^{-1}\,\mathbf{N}$ *if there exists a continuously differentiable, symmetric matrix function* $Z : \mathcal{P} \to \mathbb{R}^{n_x \times n_x}$, *such that* $\forall (p,q) \in \mathcal{P} \times \mathcal{Q}$

$$Z(p) > 0 \tag{10a}$$

$$\begin{bmatrix} \partial Z(p,q) + Z(p)\,\bar{A}(p) + \bar{A}^T(p)\,Z(p) - C^T(p)R^{-1}(p)C(p) & Z(p)\,B(p) \\ B^T(p)\,Z(p) & -S(p) \end{bmatrix} < 0 \tag{10b}$$

with $R(\rho) := I + D(\rho)D^T(\rho)$, $S(p) := I + D^T(p)D(p)$, *and* $\bar{A}(p) := (A(p) - B(p)\,S^{-1}(p)\,D^T(p)\,C(p))$. *A state space realization for* $\left[\begin{array}{cc} \mathbf{M} & \mathbf{N} \end{array}\right]$ *is*

$$\begin{bmatrix} \dot{\mu} \\ \hline \nu \end{bmatrix} = \left[\begin{array}{c|cc} A(\rho) + L(\rho)\,C(\rho) & L(\rho) & B(\rho) + L(\rho)D(\rho) \\ \hline R^{-\frac{1}{2}}(\rho)C(\rho) & R^{-\frac{1}{2}}(\rho) & R^{-\frac{1}{2}}(\rho)D(\rho) \end{array}\right] \begin{bmatrix} \mu \\ \hline y \\ -u \end{bmatrix} \tag{11}$$

where

$$L(\rho) = -(B(\rho)D^T(\rho) + Z^{-1}(\rho)\,C^T(\rho))R^{-1}(\rho). \tag{12}$$

Proof. The proof is provided in the thesis of Wood.[28] It is based on applying Theorem 1 to the state space realization (11). ∎

Note that a left coprime factorization (11) parameterizes all stabilizing output injection gains L for a given system $\mathbf{P}$.[31,32]

3 | OBSERVER-BASED MIXED SENSITIVITY CONTROL

Let $y = \begin{bmatrix}\mathbf{P_d} & \mathbf{P_u}\end{bmatrix} \begin{bmatrix} d \\ u \end{bmatrix}$ denote an LPV model of the plant in response to an input u and a disturbance d with state space realization

$$\left[\begin{array}{c} \dot{x} \\ \hline y \end{array}\right] = \left[\begin{array}{c|cc} A(\rho) & B_d(\rho) & B_u(\rho) \\ \hline C(\rho) & 0 & 0 \end{array}\right] \begin{bmatrix} x \\ d \\ u \end{bmatrix}. \tag{13}$$

The assumption that the plant model (13) is strictly proper is made as it significantly simplifies notation. All following results can be extended for models with output $y = C(\rho)\,x + D_d(\rho)\,d + D_u(\rho)\,u$ at the expense of more complicated formulae. Furthermore, many practical problems can be accurately described by strictly proper models, for example, by including actuator dynamics.

This section derives a structured observer-based output feedback controller $\mathbf{K}$ that establishes a guaranteed bound on the induced $\mathcal{L}_2$-norm of the four-block mixed sensitivity formulation shown in Figure 1 with

$$\begin{bmatrix} e \\ u \end{bmatrix} = \begin{bmatrix} -(I + \mathbf{P_u}\,\mathbf{K})^{-1}\,\mathbf{P_d} & (I + \mathbf{P_u}\,\mathbf{K})^{-1} \\ -\mathbf{K}\,(I + \mathbf{P_u}\,\mathbf{K})^{-1}\,\mathbf{P_d} & \mathbf{K}\,(I + \mathbf{P_u}\,\mathbf{K})^{-1} \end{bmatrix} \begin{bmatrix} d \\ r \end{bmatrix}. \tag{14}$$

The sensitivity $\mathbf{S} = (I + \mathbf{P_u}\,\mathbf{K})^{-1}$ represents the closed-loop error dynamics in response to a reference signal r and the disturbance sensitivity $\mathbf{S}\,\mathbf{P_d}$ represents the error dynamics in response to a disturbance d. Similarly, $\mathbf{K}\,\mathbf{S}$ and $\mathbf{K}\,\mathbf{S}\,\mathbf{P_d}$ represent the closed-loop controller action in response to these inputs, that is, the control sensitivity. In a typical practical control design problem, the inputs and outputs are frequency-weighted to represent different performance specifications. The following derivations are conducted on the unweighted problem (14) to simplify notation. Weights are subsequently introduced in Section 3.3. Removing the controller $\mathbf{K}$ from the interconnection in Figure 1 yields the open-loop generalized plant

$$\left[\begin{array}{c} \dot{x} \\ \hline e \\ u \\ e \end{array}\right] = \left[\begin{array}{c|ccc} A(\rho) & B_d(\rho) & 0 & B_u(\rho) \\ \hline -C(\rho) & 0 & I & 0 \\ 0 & 0 & 0 & I \\ -C(\rho) & 0 & I & 0 \end{array}\right] \begin{bmatrix} x \\ d \\ r \\ u \end{bmatrix}. \tag{15}$$

Its structure matches Equation (5) and a dynamic output feedback LPV controller can be obtained directly as described in Section 2.1. Instead, an approach is proposed in the following section that separates the synthesis procedure into two steps: an observer synthesis and a state feedback synthesis. For LTI systems, this separation is well known.[10] For LPV systems, separation was addressed only recently by Prempain and Postlethwaite[15,18] as well as by Saupe and Pfifer.[19] Prempain and Postlethwaite use a coprime factorization approach to split the controller synthesis problem into an observer and state feedback design problem. They start with designing an $\mathcal{H}_2$-optimal observer and then use open loop shaping[33-35] to design a state feedback controller. Saupe and Pfifer perform induced $\mathcal{L}_2$-norm optimal observer and state feedback designs, but treat the design problems as independent. As the observer design has a major influence on the achievable performance, their method relies heavily on nonlinear optimization of weighting functions. Both approaches lose the connection to classical mixed sensitivity design, which complicates tuning. By contrast, the following results show how separate design problems are formulated in a way that retains the standard mixed sensitivity structure and its ease of tuning.

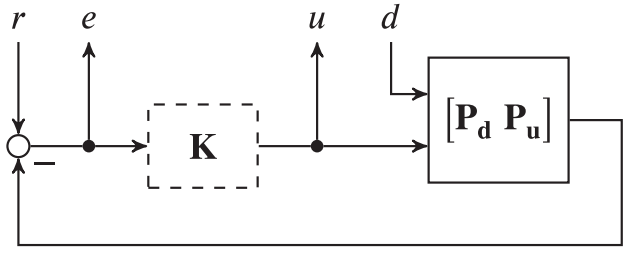

FIGURE 1 Mixed sensitivity four-block problem

3.1 | Loop properties of observer-based control

The structure of the observer-based output feedback controller $\mathbf{K}$ in this article is fixed to the form

$$\begin{bmatrix} \dot{\xi} \\ u \end{bmatrix} = \left[\begin{array}{c|c} A(\rho) + B_u(\rho)F(\rho) + L(\rho)C(\rho) & L(\rho) \\ \hline F(\rho) & 0 \end{array}\right] \begin{bmatrix} \xi \\ e \end{bmatrix}, \tag{16}$$

where L is the observer (output injection) gain and F is the state feedback gain. Note that this form is different from the standard observer form of LPV and $\mathcal{H}_\infty$-controllers.[26,28,36] Given the structure (16), the controller $\mathbf{K}$ can be split into a dynamic part, the observer $\mathbf{O}$, with state space realization

$$\begin{bmatrix} \dot{\xi} \\ \xi \end{bmatrix} = \left[\begin{array}{c|cc} A(\rho) + L(\rho)C(\rho) & L(\rho) & B_u(\rho) \\ \hline I & 0 & 0 \end{array}\right] \begin{bmatrix} \xi \\ e \\ u \end{bmatrix}, \tag{17}$$

and a static part $\mathbf{F}$, the state feedback law

$$u = F(\rho)\,\xi. \tag{18}$$

Note that substituting the state feedback law (18) into the observer (17) immediately recovers the output feedback controller (16). With the structured controller, the mixed sensitivity problem in Figure 1 can be restated as depicted in Figure 2. The following derivation establishes that an equivalent representation of the mixed sensitivity problem is given by the combination of the two problems depicted in Figure 3. The link between these problems is provided by a contractive left coprime factorization $\mathbf{M}^{-1}[\mathbf{N_d}\ \mathbf{N_u}] = [\mathbf{P_d}\ \mathbf{P_u}]$ of the plant model.

The input of a single-degree-of-freedom output feedback controller is the control error $e = r - y$, not the plant output y. As a consequence, the observer state ξ does not represent an estimate of the plant's state x, but rather an *error state*. Hence, it is justified to define the output estimation error

$$\hat{e} = C(\rho)\,\xi - (y - r) = C(\rho)\,\xi + e \tag{19}$$

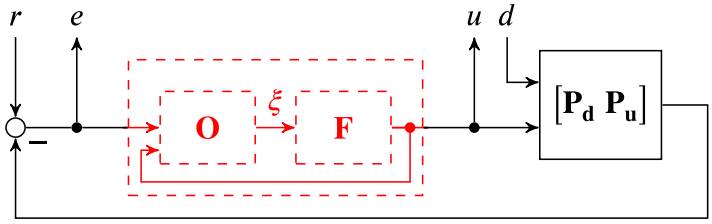

FIGURE 2 Mixed sensitivity four-block problem with observer-based controller [Colour figure can be viewed at wileyonlinelibrary.com]

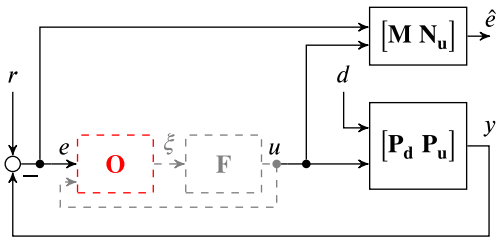

(A) Observer design problem with minimal state space realization (22) independent of $\mathbf{F}$

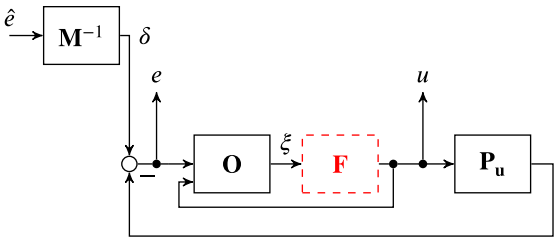

(B) State feedback design problem with minimal state space realization (27) for given observer $\mathbf{O}$

FIGURE 3 Rearranged mixed sensitivity four-block problem with output estimation/state feedback separation [Colour figure can be viewed at wileyonlinelibrary.com]

instead of the commonly used state estimation error $\epsilon = \xi - x$. It is next shown that the output estimation error $\hat{e}$ is completely independent of the choice of the state feedback law $\mathbf{F}$. First, a state space representation for $\begin{bmatrix} r \\ d \end{bmatrix} \to \hat{e}$ in Figure 3A is derived. Combining the state space equations of the plant model (13), the structured controller (16), and the definition of the output estimation error in Equation (19), it follows

$$\begin{bmatrix} \dot{x} \\ \dot{\xi} \\ \hat{e} \end{bmatrix} = \left[\begin{array}{cc|cc} A(\rho) & B_u(\rho)F(\rho) & B_d(\rho) & 0 \\ -L(\rho)C(\rho) & A(\rho)+B_u(\rho)F(\rho)+L(\rho)C(\rho) & 0 & L(\rho) \\ \hline -C(\rho) & C(\rho) & 0 & I \end{array}\right] \begin{bmatrix} x \\ \xi \\ d \\ r \end{bmatrix}. \tag{20}$$

Using the state space coordinate transformation $\epsilon = \xi - x$ turns Equation (20) into

$$\begin{bmatrix} \dot{\epsilon} \\ \dot{\xi} \\ \hat{e} \end{bmatrix} = \left[\begin{array}{cc|cc} A(\rho)+L(\rho)C(\rho) & 0 & -B_d(\rho) & L(\rho) \\ L(\rho)C(\rho) & A(\rho)+B_u(\rho)F(\rho) & 0 & L(\rho) \\ \hline C(\rho) & 0 & 0 & I \end{array}\right] \begin{bmatrix} \epsilon \\ \xi \\ d \\ r \end{bmatrix}. \tag{21}$$

Thus, the controller state ξ is unobservable from the estimation error $\hat{e}$. For any admissible state feedback gain, $A(\rho)+B(\rho)F(\rho)$ is stable and ξ can be removed to obtain the equivalent realization

$$\begin{bmatrix} \dot{\epsilon} \\ \hat{e} \end{bmatrix} = \left[\begin{array}{c|cc} A(\rho)+L(\rho)C(\rho) & -B_d(\rho) & L(\rho) \\ \hline C(\rho) & 0 & I \end{array}\right] \begin{bmatrix} \epsilon \\ d \\ r \end{bmatrix}. \tag{22}$$

Equation (22) is a state space realization of $[-\mathbf{N_d}\ \mathbf{M}]$ with $\mathbf{M}^{-1}[\mathbf{N_d}\ \mathbf{N_u}] = [\mathbf{P_d}\ \mathbf{P_u}]$ when L is selected in accordance with Theorem 4. Hence, the estimation error can be expressed as

$$\hat{e} = \mathbf{M}\, r - \mathbf{N_d}\, d \tag{23}$$

with $\|\mathbf{M}\| \le 1$ and $\|\mathbf{N_d}\| \le 1$. Note that $\mathbf{M}$ has high-pass characteristics and connects the reference signal to the output estimation error. Hence, it plays the role of a sensitivity function for the estimation problem. Conversely, $\mathbf{N_d}$ has, in general, low-pass properties and describes how disturbances affect the estimation error. It plays the role of a disturbance sensitivity for the estimation problem. The contractive left coprime factorization thus parameterizes all observer gains L that result in peak sensitivities less than one; a corollary of the well-known result[31,32] that L parameterizes all left coprime factorizations.

It is next shown that the relation (23) indeed establishes the link between the output estimation problem of Figure 3A and the state feedback problem of Figure 3B. Specifically, Equation (23) states that $\mathbf{M}^{-1}\ \hat{e} = r - \mathbf{P_d}\ d$. Consequently, the input $r - \mathbf{P_d}\, d$ in Figure 3A can be replaced by a fictitious disturbance $\delta = \mathbf{M}^{-1}\ \hat{e}$ as done in Figure 3B. The state space realization for $\mathbf{M}^{-1}$ is calculated from Equation (22) as

$$\begin{bmatrix} \dot{\zeta} \\ \delta \end{bmatrix} = \left[\begin{array}{c|c} A(\rho) & L(\rho) \\ \hline -C(\rho) & I \end{array}\right] \begin{bmatrix} \zeta \\ \hat{e} \end{bmatrix}. \tag{24}$$

It depends only on the choice of L and the plant model. A complete state space realization of the open-loop generalized plant in Figure 3B, including the input weight $\mathbf{M}^{-1}$ and the observer $\mathbf{O}$ is

$$\begin{bmatrix} \dot{x} \\ \dot{\zeta} \\ \dot{\xi} \\ e \\ u \\ \xi \end{bmatrix} = \left[\begin{array}{ccc|cc} A(\rho) & 0 & 0 & 0 & B_u(\rho) \\ 0 & A(\rho) & 0 & L(\rho) & 0 \\ -L(\rho)C(\rho) & -L(\rho)C(\rho) & A(\rho)+L(\rho)C(\rho) & L(\rho) & B_u(\rho) \\ \hline -C(\rho) & -C(\rho) & 0 & I & 0 \\ 0 & 0 & 0 & 0 & I \\ 0 & 0 & I & 0 & 0 \end{array}\right] \begin{bmatrix} x \\ \zeta \\ \xi \\ \hat{e} \\ u \end{bmatrix}. \tag{25}$$

Note that the estimation error $\hat{e}$ is the only external disturbance and that the available feedback signal is the complete observer state ξ. Using the coordinate transformation $\varepsilon = \xi - (x + \zeta)$ on Equation (25) yields

$$\left[\begin{array}{c} \dot{\epsilon} \\ \dot{\zeta} \\ \dot{\xi} \\ \hline e \\ u \\ \xi \end{array}\right] = \left[\begin{array}{ccc|cc} A(\rho)+L(\rho)C(\rho) & 0 & 0 & 0 & 0 \\ 0 & A(\rho) & 0 & L(\rho) & 0 \\ L(\rho)C(\rho) & 0 & A(\rho) & L(\rho) & B_u(\rho) \\ \hline C(\rho) & 0 & -C(\rho) & I & 0 \\ 0 & 0 & 0 & 0 & I \\ 0 & 0 & I & 0 & 0 \end{array}\right] \left[\begin{array}{c} \epsilon \\ \zeta \\ \xi \\ \hline \hat{e} \\ u \end{array}\right]. \tag{26}$$

Thus, ϵ is uncontrollable and ζ is unobservable. Removing these states yields the equivalent realization

$$\left[\begin{array}{c} \dot{\xi} \\ \hline e \\ u \\ \xi \end{array}\right] = \left[\begin{array}{c|cc} A(\rho) & L(\rho) & B_u(\rho) \\ \hline -C(\rho) & I & 0 \\ 0 & 0 & I \\ I & 0 & 0 \end{array}\right] \left[\begin{array}{c} \xi \\ \hat{e} \\ u \end{array}\right]. \tag{27}$$

The measured output available to the controller is the complete state vector ξ of the realization (27) such that the controller synthesis problem can be solved by state feedback.[10,28,37,38] Once the state feedback gain is obtained, the output feedback controller (16) is known and the resultant closed loop $\hat{e} \to \begin{bmatrix} e \\ u \end{bmatrix}$ is

$$\begin{bmatrix} e \\ u \end{bmatrix} = \begin{bmatrix} (I + \mathbf{P_u}\,\mathbf{K})^{-1} \\ \mathbf{K}\,(I + \mathbf{P_u}\,\mathbf{K})^{-1} \end{bmatrix} \mathbf{M}^{-1}\,\hat{e}. \tag{28}$$

It is readily verified that substitution of Equation (23) into Equation (28) yields Equation (14). That is, the combination of the input-output maps $\begin{bmatrix} r \\ d \end{bmatrix} \to \hat{e}$ and $\hat{e} \to \begin{bmatrix} e \\ u \end{bmatrix}$ indeed retains the mixed sensitivity input-output map (14). More specifically, it is shown in the following theorem that the output estimation/state feedback separation of Figure 3 provides a guaranteed performance bound for the output feedback mixed sensitivity problem of Figure 2.

Theorem 5 (observer-based controller synthesis). *Let $\mathcal{P}$ and $\mathcal{Q}$ be given compact sets and $\mathbf{G}$ an LPV system (15). There exists an observer-based controller $\mathbf{K}$ as in Equation (16) such that $\|\mathcal{F}(\mathbf{G},\mathbf{K})\| \le \gamma$ if there exist continuously differentiable, symmetric matrix functions $Z : \mathcal{P} \to \mathbb{R}^{n_x \times n_x}$ and $Y : \mathcal{P} \to \mathbb{R}^{n_x \times n_x}$ such that $\forall (p,q) \in \mathcal{P} \times \mathcal{Q}$*

$$Z(p) > 0 \tag{29a}$$

$$\begin{bmatrix} \partial Z(p,q) + Z(p)\,A(p) + A^T(p)\,Z(p) - C^T(p)C(p) & Z(p)\,B_d(p) \\ B_d^T(p)\,Z(p) & -I \end{bmatrix} < 0 \tag{29b}$$

and

$$\gamma > 1 \tag{30a}$$

$$Y(p) > 0 \tag{30b}$$

$$\begin{bmatrix} Y(p)A^T(p) + A(p)Y(p) - \partial Y(p,q) - \gamma B_u(p)B_u^T(p) & -Y(p)C^T(p) & -Z^{-1}(p)C^T(p) \\ -C(p)Y(p) & -\gamma I & I \\ -C(p)Z^{-1}(p) & I & -\gamma I \end{bmatrix} < 0. \tag{30c}$$

Proof. Equations (29) are the existence conditions of Theorem 4 for the contractive left coprime factorization $\mathbf{M}^{-1}\,\mathbf{N_d} = \mathbf{P_d}$. They yield the observer gain $L(p) = -Z^{-1}(p)\,C^T(p)$ and establish Equation (23). Equations (30) are the state feedback existence conditions of Theorem 3 for the generalized plant (27). They yield $F(p) = -\gamma\ B_u^T(p)\ Y^{-1}(p)$ and

establish Equation (28). It was previously shown that the combination of Equations (23) and (28) recovers the original mixed sensitivity problem (14). The property $\|[\mathbf{M}\ \mathbf{N_d}]\| \leq 1$ of the contractive coprime factorization implies $\|[-\mathbf{N_d}\ \mathbf{M}]\| \leq 1$ and it follows from submultiplicativity of the induced $\mathcal{L}_2$-norm that

$$\begin{aligned}\left\| \begin{bmatrix} -\mathbf{S}\mathbf{P_d} & \mathbf{S} \\ -\mathbf{K}\,\mathbf{S}\mathbf{P_d} & \mathbf{K}\,\mathbf{S} \end{bmatrix} \right\| = \left\| \begin{bmatrix} \mathbf{S} \\ \mathbf{K}\,\mathbf{S} \end{bmatrix} \mathbf{M}^{-1} \begin{bmatrix} -\mathbf{N_d} & \mathbf{M} \end{bmatrix} \right\| &\leq \left\| \begin{bmatrix} \mathbf{S} \\ \mathbf{K}\,\mathbf{S} \end{bmatrix} \mathbf{M}^{-1} \right\| \|[-\mathbf{N_d}\ \mathbf{M}]\| \\ &\leq \left\| \begin{bmatrix} \mathbf{S} \\ \mathbf{K}\,\mathbf{S} \end{bmatrix} \mathbf{M}^{-1} \right\|. \end{aligned} \tag{31}$$

■

The important implication of Theorem 5 is that the existence conditions (29) for the observer and (30) for the state feedback gain are coupled in only one direction. That is, first an observer can be obtained from (29) and subsequently a state feedback gain can be calculated from (30). These two steps are computationally significantly less expensive than the single computation required to obtain an output feedback controller from the conditions (7) of Theorem 2.

3.2 | Conservatism and optimal choice of the observer gain

The previous section established guaranteed closed-loop performance of the two-step synthesis. First, a contractive left coprime factorization is calculated to obtain an observer gain. Subsequently, a particular state feedback problem that includes the observer is solved. Naturally, the question arises, how conservative this two-step synthesis is. For LTI systems, a famous $\mathcal{H}_\infty$-loopshaping result by Glover and McFarlane[33,35] states that the inequality (31) becomes an equality when the observer gain is selected such that the coprime factorization $\begin{bmatrix}\mathbf{M} & \mathbf{N_d}\end{bmatrix}$ is coinner, that is, when $\begin{bmatrix}\mathbf{M} & \mathbf{N_d}\end{bmatrix}\ \begin{bmatrix}\mathbf{M} & \mathbf{N_d}\end{bmatrix}^* = I$ with $*$ denoting the adjoint operator, see Zhou et al[10] for details. In this case, the observer gain is unique and there is no conservatism associated with the two-step procedure. For LPV systems, there exists no notion of a coinner coprime factorization. The contractive coprime factorization (29) guarantees $\|[\mathbf{M}\ \mathbf{N_d}]\| \leq 1$, but does not uniquely determine an observer gain. Consequently, some conservatism related to the choice of the observer gain is expected.

The main result in this section shows that the observer gain can indeed be selected such that the search space for the solution of the subsequent state feedback synthesis conditions (30) is maximized which, conversely, minimizes conservatism. To show this, an actual state feedback problem, that is, all state variables can be measured, is considered for comparison. Let the mixed sensitivity problem with generalized plant (15) specify the performance requirements. The actual state feedback problem for this generalized plant in accordance with Theorem 3 is finding a continuously differentiable, symmetric matrix function $Y : \mathcal{P} \to \mathbb{R}^{n_x \times n_x}$ such that $\forall (p, q) \in \mathcal{P} \times \mathcal{Q}$

$$\gamma > 1 \tag{32a}$$

$$Y(p) > 0 \tag{32b}$$

$$\begin{bmatrix} Y(p)A^T(p) + A(p)Y(p) - \partial Y(p,q) - \gamma B_u(p)B_u^T(p) & Y(p)C^T(p) & B_d(p) & 0 \\ C(p)Y(p) & -\gamma I & 0 & I \\ B_d(p)^T & 0 & -\gamma I & 0 \\ 0 & I & 0 & -\gamma I \end{bmatrix} < 0. \tag{32c}$$

This actual state feedback problem provides a lower bound on the achievable performance of an observer-based controller.[10,38] Comparing the feasible sets of the actual state feedback synthesis condition (32) and the observer-based state feedback synthesis condition (30) provides a measure of how much conservatism is introduced by using an observer. To allow such a comparison, the condition (32c) is reformulated using the Schur complement argument

$$\begin{bmatrix} S_{11} & S_{12} \\ S_{12}^T & S_{22} \end{bmatrix} < 0 \iff S_{11} < 0 \ \text{ and } \ S_{11} - S_{12}S_{22}^{-1}S_{12}^T < 0.$$

With $S_{11} = Y\,A^T + A\,Y - \partial Y - \gamma\,B_u\,B_u^T$, it follows

$$Y\,A^T + A\,Y - \partial Y - \gamma\,B_u\,B_u^T + \frac{1}{\gamma}\,B_d\,B_d^T - \frac{\gamma}{1-\gamma^2}\,Y\,C^T\,C\,Y < 0. \tag{33}$$

Assume now that a feasible solution (Z_0, Y_0, γ_0) for the observer-based synthesis conditions (29) and (30) is found. Applying the Schur complement argument with $S_{11} = Y_0\,A^T + A\,Y_0 - \partial Y_0 - \gamma_0\,B_u\,B_u^T$ on condition (30c) shows that this solution also satisfies

$$Y_0\,A^T + A\,Y_0 - \partial Y_0 - \gamma_0\,B_u\,B_u^T + \frac{1}{\gamma_0}Z_0^{-1}\,C^T\,C\,Z_0^{-1} - \frac{\gamma_0}{1-\gamma_0^2}\left(Y_0 + \frac{1}{\gamma_0}Z_0^{-1}\right)C^TC\left(Y_0 + \frac{1}{\gamma_0}Z_0^{-1}\right) < 0. \tag{34}$$

The Schur complement of condition (29b) further implies

$$Z_0^{-1}\,A^T + A\,Z_0^{-1} - \partial Z_0^{-1} + B_d\,B_d^T < Z_0^{-1}\,C^T\,C\,Z_0^{-1}. \tag{35}$$

Using the inequality (35), $Z_0^{-1}\,C^T\,C\,Z_0^{-1}$ in inequality (34) can be replaced with $Z_0^{-1}\,A^T + A\,Z_0^{-1} - \partial Z_0^{-1} + B_d\,B_d^T$. Hence, the particular solution (Z_0, Y_0, γ_0) also satisfies

$$\begin{aligned}\left(Y_0 + \frac{1}{\gamma_0}Z_0^{-1}\right)A^T + A\left(Y_0 + \frac{1}{\gamma_0}Z_0^{-1}\right) - \partial\left(Y_0 + \frac{1}{\gamma_0}Z_0^{-1}\right) - \gamma_0\,B_u\,B_u^T + \frac{1}{\gamma_0}B_d\,B_d^T \\ - \frac{\gamma_0}{1-\gamma_0^2}\left(Y_0 + \frac{1}{\gamma_0}Z_0^{-1}\right)C^TC\left(Y_0 + \frac{1}{\gamma_0}Z_0^{-1}\right) < 0.\end{aligned} \tag{36}$$

Comparing inequality (36) with (33) shows that *any* feasible solution (Z_0, Y_0, γ_0) of the observer-based state feedback synthesis is also a feasible solution of (33) by setting $Y = Y_0 + \frac{1}{\gamma_0}Z_0^{-1}$. Conversely, a particular feasible solution (Y_*, γ_0) of the actual state feedback condition (33) satisfies (36) with $Y_0 = Y_* - \frac{1}{\gamma_0}\,Z_0^{-1}$, but is in general *not* a feasible solution of the observer-based conditions (30) since $Y_* - \frac{1}{\gamma_0}\,Z_0^{-1}$ is not necessarily positive definite. Hence, the feasible solutions for the observer-based state feedback synthesis conditions (30) form a strict subset of the feasible solutions for the actual state feedback synthesis conditions (32). From convexity, it follows that the achievable performance of the observer-based controller is limited by the feasibility gap, that is, the difference between these sets. The feasibility gap is completely characterized by the term $\frac{1}{\gamma_0}Z_0^{-1}$. As $Z^{-1} \to 0$, the feasible set of the observer-based synthesis conditions converges toward the feasible set of the actual state feedback synthesis conditions. This observation motivates the following semidefinite program to obtain the observer gain: Among the set of contractive left coprime factorizations, use the one with minimum trace(Z^{-1}). This is achieved by introducing a slack variable $W \in \mathbb{R}^{n_x \times n_x}$ and minimizing trace(W) subject to (29) and the additional constraint $\forall p \in \mathcal{P}$

$$\begin{bmatrix} W & I \\ I & Z(p) \end{bmatrix} > 0. \tag{37}$$

The constraint (37) ensures $W - Z^{-1} > 0$ by Schur complement and consequently trace$(W) >$ trace(Z^{-1}). Note that Prempain and Postlethwaite[15] suggest the same objective and interpret it as an $\mathcal{H}_2$-optimal observer design at frozen parameter values $\rho(t)$. The interpretation provided in this section complements the one given by Prempain and Postlethwaite[15] and shows that their way of calculating an observer actually leads to optimal performance given the structural constraints of the controller. Finally, as $L(p) = -Z^{-1}(p)\,C^T(p)$, the optimization can also be understood as directly minimizing the observer gain.

3.3 | Design and synthesis procedure

In the previous section, the unweighted problem was considered to ease the derivation. For any sensible practical control design problem, it is important to introduce weights. Specifically, the following weighting structure, depicted in Figure 4, is considered for the mixed sensitivity four-block problem:

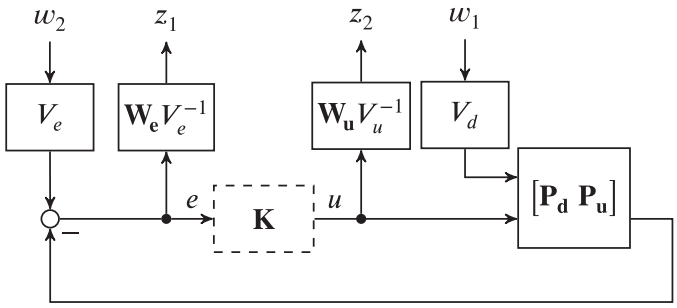

FIGURE 4 Weighted mixed sensitivity problem

$$\begin{bmatrix} z_1 \\ z_2 \end{bmatrix} = \begin{bmatrix} \mathbf{W_e}V_e^{-1} & 0 \\ 0 & \mathbf{W_u}V_u^{-1} \end{bmatrix} \begin{bmatrix} -\mathbf{S}\,\mathbf{P_d} & \mathbf{S} \\ -\mathbf{K}\,\mathbf{S}\,\mathbf{P_d} & \mathbf{K}\,\mathbf{S} \end{bmatrix} \begin{bmatrix} V_d & 0 \\ 0 & V_e \end{bmatrix} \begin{bmatrix} w_1 \\ w_2 \end{bmatrix}. \tag{38}$$

The design procedure for an observer-based output feedback LPV controller consists of four steps: weight selection, observer synthesis, state feedback synthesis, and controller assembly. Each step is summarized in the following.

Step 1: Selection of the weighting functions. The formulation (38) was introduced by Theis[39] as a particular easy way of tuning mixed sensitivity controllers. It separates the weighting into frequency-dependent parts, denoted $\mathbf{W}$, and static parts, denoted V. Each of the weights is diagonal and thus relates to physical inputs and outputs with a clear interpretation. The weighting filter $\mathbf{W_e}$ determines the shape of the sensitivity and disturbance sensitivity functions. It represents requirements on sensitivity reduction and is usually selected with integral behavior up to the desired closed-loop bandwidth and gain 0.5 beyond that frequency for tracked outputs and as a unit gain for additional feedback signals. Doing so, sensitivity is reduced up the desired closed-loop bandwidth and sensitivity degradation beyond that frequency is limited to a factor of 2. The weighting filter $\mathbf{W_u}$ determines the shape of the control sensitivity and represents actuator limitations and robustness requirements. It is usually selected with unit gain up to the available control bandwidth and differentiating behavior beyond that frequency to enforce controller roll-off. Other possible choices include inverse bandpass filters or notch filters to allocate a specific frequency region for control activity. Once the weighting filters are fixed, tuning can be performed purely based on the diagonal static weights V_e, V_u, and V_d. They can be assigned the interpretation of maximum values for errors, control signals, and disturbances, respectively. Hence, it is often possible to find good initial values based on physical insight into the problem. For example, V_e is often selected as the maximum expected command value for tracked-outputs and such that cross-coupling into other channels due to this command is equally acceptable. The weight V_u is selected to represent available control action relative to the previously specified maximum errors and also relative to maximum disturbances as specified through V_d. Thus, V_u is often selected based on the physical saturation limits of the actuators. Depending on the specific disturbance model $\mathbf{P_d}$, values for V_d are often found from physical insight into the maximum expected value of disturbances. When load disturbances ($\mathbf{P_d} = \mathbf{P_u}$) are considered, another useful interpretation of the ratio of V_d and V_u is uncertainty in the input channels. Furthermore, as Section 3.3 shows, the size of V_d relative to V_e directly determines the relative contribution of the second column to the optimization problem. Hence, V_d trades off disturbance rejection capabilities (through $\mathbf{S}\,\mathbf{P_d}$) vs tracking performance (through $\mathbf{S}$). While the tuning process remains iterative and interactive, it is often easy and fast to find suitable values in this way. For an extensive design study and further details on weight selection, the reader is referred to Theis et al.[40]

Step 2: Observer synthesis. The observer is obtained by calculating a contractive left coprime factorization $\mathbf{M}^{-1}\,\mathbf{N_d}$ of the *scaled* disturbance model $V_e^{-1}\ \mathbf{P_d}\ V_d$. Solving the SDP

$$\min_{Z(p),W} \operatorname{trace}(W) \quad \text{s. t. } \forall (p,q) \in \mathcal{P} \times \mathcal{Q}$$

$$\begin{bmatrix} W & I \\ I & Z(p) \end{bmatrix} > 0 \tag{39a}$$

$$\begin{bmatrix} \partial Z(p,q) + Z(p)A(p) + A^T(p)Z(p) - C^T(p)V_e^{-2}(p)C(p) & Z(p)B_d(p)V_d(p) \\ V_d^T(p)B_d^T(p)Z(p) & -I \end{bmatrix} < 0 \tag{39b}$$

yields the observer gain

$$L(\rho) = -Z^{-1}(\rho)\ C^T(\rho)V_e^{-1}(\rho). \tag{40}$$

As described in Section 3.2, this SDP maximizes the feasibility region for the subsequent state feedback synthesis. Note that the observer synthesis depends only on the choice of the static weights V_e and V_d.

Step 3: State feedback synthesis. To obtain the state feedback gain, a weighted version of Equation (28) is used. The observer gain from step 2 defines an input weight $\mathbf{M}^{-1}$ based on the *scaled* disturbance model. Thus, an additional factor V_e needs to be included to recover the mixed sensitivity formulation (38) as

$$\begin{bmatrix} z_1 \\ z_2 \end{bmatrix} = \begin{bmatrix} \mathbf{W_e} V_e^{-1} & 0 \\ 0 & \mathbf{W_u} V_u^{-1} \end{bmatrix} \begin{bmatrix} \mathbf{S} \\ \mathbf{KS} \end{bmatrix} V_e \, \mathbf{M}^{-1} \begin{bmatrix} -\mathbf{N_d} & \mathbf{M} \end{bmatrix} \begin{bmatrix} w_1 \\ w_2 \end{bmatrix}.$$

As such, the weighted version of Equation (28) is

$$\begin{bmatrix} z_1 \\ z_2 \end{bmatrix} = \begin{bmatrix} \mathbf{W_e} V_e^{-1} & 0 \\ 0 & \mathbf{W_u} V_u^{-1} \end{bmatrix} \begin{bmatrix} \mathbf{S} \\ \mathbf{KS} \end{bmatrix} V_e \, \mathbf{M}^{-1} \, \hat{e}.$$

It remains to explicitly give the SDP to calculate the state feedback gain $F(\rho)$. Denote the state space realizations of the weighting filters $\mathbf{W_e}$ and $\mathbf{W_u}$, respectively, by

$$\left[\begin{array}{c} z_1 \\ \hline \dot{\xi}_{We} \end{array}\right] = \left[\begin{array}{c|c} A_{We}(\rho) & B_{We}(\rho) \\ \hline C_{We}(\rho) & D_{We}(\rho) \end{array}\right] \left[\begin{array}{c} \xi_{We} \\ \hline e \end{array}\right] \qquad \text{and} \qquad \left[\begin{array}{c} z_2 \\ \hline \dot{\xi}_{Wu} \end{array}\right] = \left[\begin{array}{c|c} A_{Wu}(\rho) & B_{Wu}(\rho) \\ \hline C_{Wu}(\rho) & D_{Wu}(\rho) \end{array}\right] \left[\begin{array}{c} \xi_{Wu} \\ \hline u \end{array}\right]. \tag{41}$$

Introducing a scaled control input $\hat{u} = D_{Wu} \, V_u^{-1} \, u$ in order to satisfy the normalized structure of Equation (5), the open-loop generalized plant for the state feedback synthesis is

$$\left[\begin{array}{c} \dot{\xi} \\ \dot{\xi}_{We} \\ \dot{\xi}_{Wu} \\ \hline z_1 \\ z_2 \end{array}\right] = \left[\begin{array}{ccc|cc} A(\rho) & 0 & 0 & L(\rho) & B_u(\rho) V_u(\rho) D_{Wu}^{-1}(\rho) \\ -B_{We}(\rho) \, V_e^{-1}(\rho) \, C(\rho) & A_{We}(\rho) & 0 & B_{We}(\rho) & 0 \\ 0 & 0 & A_{Wu}(\rho) & 0 & B_{Wu}(\rho) \, D_{Wu}^{-1}(\rho) \\ \hline 0 & C_{We}(\rho) & 0 & D_{We}(\rho) & 0 \\ 0 & 0 & C_{Wu}(\rho) & 0 & I \end{array}\right] \left[\begin{array}{c} \xi \\ \xi_{We} \\ \xi_{Wu} \\ \hat{e} \\ \hat{u} \end{array}\right]. \tag{42}$$

With L known from the previous step and using the abbreviation

$$\left[\begin{array}{c} \dot{\xi} \\ \dot{\xi}_{We} \\ \dot{\xi}_{Wu} \\ \hline z_1 \\ z_2 \end{array}\right] = \left[\begin{array}{c|cc} A_{\mathrm{SF}}(\rho) & B_{\mathrm{SF},11}(\rho) & B_{\mathrm{SF},2}(\rho) \\ \hline C_{\mathrm{SF},11}(\rho) & D_{\mathrm{SF},1111}(\rho) & 0 \\ C_{\mathrm{SF},12}(\rho) & 0 & I \end{array}\right] \left[\begin{array}{c} \xi \\ \xi_{We} \\ \xi_{Wu} \\ \hline \hat{e} \\ \hat{u} \end{array}\right] \tag{43}$$

for the state space representation (42), the following SDP in accordance with Theorem 3 is solved:

$$\min_{Y(p),\gamma} \gamma \text{ s. t. } \forall (p,q) \in \mathcal{P} \times \mathcal{Q}$$

$$\gamma > 1 \tag{44a}$$

$$Y(p) > 0 \tag{44b}$$

$$\begin{bmatrix} Y(p) A_{\mathrm{SF}}^T(p) + A_{\mathrm{SF}}(p) Y(p) - \partial Y(p,q) - \gamma B_{\mathrm{SF},2}(p) B_{\mathrm{SF},2}^T(p) & -Y(p) C_{\mathrm{SF},11}^T(p) & B_{\mathrm{SF},11}(p) \\ -C_{\mathrm{SF},11}(p) Y(p) & -\gamma I & D_{\mathrm{SF},1111}(p) \\ B_{\mathrm{SF},11}^T(p) & D_{\mathrm{SF},1111}(p) & -\gamma I \end{bmatrix} < 0. \tag{44c}$$

The state feedback gain is then calculated from Equation (9) and by reversing the scaling as

$$F(\rho) = -V_u(\rho) \, D_{Wu}^{-1}(\rho) \, (\gamma \, B_{\mathrm{SF},2}^T(\rho) \, Y^{-1}(\rho) + C_{\mathrm{SF},12}(\rho)). \tag{45}$$

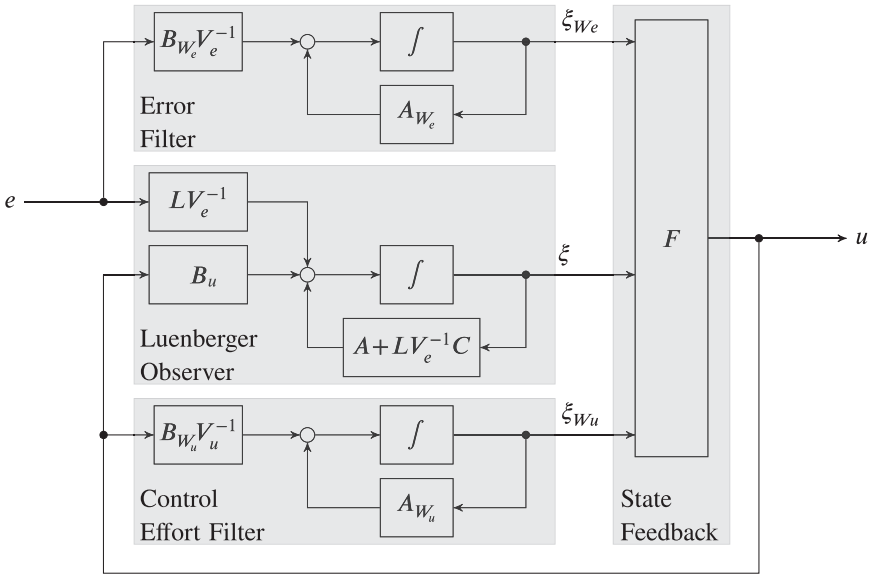

FIGURE 5 Observer-based controller for weighted mixed sensitivity problem

Note that the disturbance model and the weight V_d enter the problem only indirectly through the particular observer gain L.

Step 4: Controller assembly. The resulting observer-based LPV controller is highly structured. It consists of the observer, the state feedback gain, and the weighting filters as depicted in Figure 5.

Often, $\mathbf{W_e}$ contains only integral dynamics, that is, $A_{We} = 0$. In this case, the integrators appear explicitly in the error filter, which can be exploited in implementation, for example, to include simple antiwindup compensation.[24] A state space representation for the complete observer-based controller is

$$\begin{bmatrix} \dot{\xi} \\ \dot{\xi}_{We} \\ \dot{\xi}_{Wu} \\ \hline u \end{bmatrix} = \left[\begin{array}{ccc|c} A(\rho)+L(\rho)\,V_e^{-1}(\rho)\,C(\rho) & 0 & 0 & \begin{matrix} B_u(\rho)\,F(\rho) \\ 0 \\ B_{Wu}(\rho)\,V_u^{-1}(\rho)\,F(\rho) \end{matrix} \\ 0 & A_{We}(\rho) & 0 & \begin{matrix} L(\rho)\,V_e^{-1}(\rho) \\ B_{We}(\rho)\,V_e^{-1}(\rho) \\ 0 \end{matrix} \\ 0 & 0 & A_{Wu}(\rho) & \\ \hline F(\rho) & & & 0 \end{array}\right] \begin{bmatrix} \xi \\ \xi_{We} \\ \xi_{Wu} \\ \hline e \end{bmatrix}. \tag{46}$$

4 | APPLICATION EXAMPLE: CONTROL OF A UAV BEYOND FLUTTER SPEED

A representative model of NASA's X56A Multiutility Technology Testbed (MUTT) aircraft, depicted in Figure 6, is used to demonstrate the effectiveness of the proposed synthesis technique. The X56A is a research platform for control of highly flexible aircraft and flutter suppression.[41] A mathematical model of the X56A aircraft was developed by Schulze et al[42] combining rigid-body flight dynamics from first principle modeling, structural dynamics from FEM modeling, and unsteady aerodynamics from CFD modeling. This high-fidelity model builds the basis for the following design example.

In this article, only the longitudinal dynamics of the X56A are considered. They consist of the rigid-body dynamics described by angle of attack and pitch rate, as well as the first eight flexible modes described in terms of their modal displacements. Unsteady aerodynamics states, included in the model of Schulze et al,[42] are residualized for this example. Doing so keeps the problem size small enough to be conveniently handled by conventional synthesis algorithms. As inputs, symmetric deflection of the two outboard wing flaps (δ_{O}) and the two body flaps (δ_{B}), highlighted in Figure 6, are considered. The outputs are a pitch rate measurement q and vertical acceleration signal at the center body (a_{center}), as well as a fore and aft wing tip acceleration signal ($a_{\mathrm{wing,fore}}$ and $a_{\mathrm{wing,aft}}$) as also indicated in Figure 6. Furthermore, second-order actuator dynamics are included.

The dynamics of the aircraft depend nonlinearly on the airspeed V_∞, and the state space representation is of the form

$$\begin{aligned} \dot{x} &= A(V_\infty)\,x + B(V_\infty)\,u \\ y &= C(V_\infty)\,x \end{aligned} \tag{47}$$

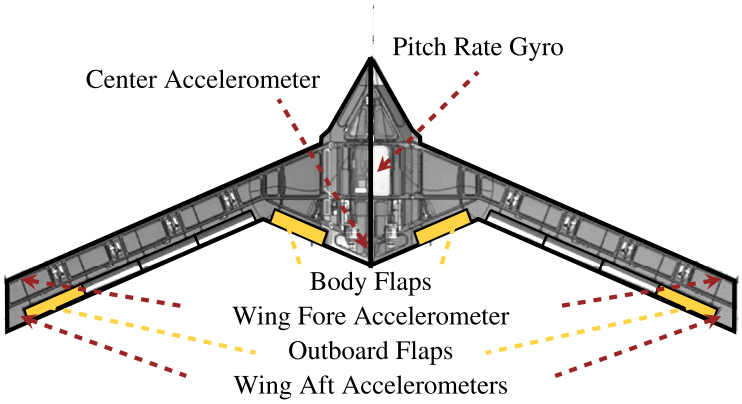

FIGURE 6 X56A MUTT unmanned aerial vehicle [Colour figure can be viewed at wileyonlinelibrary.com]

with state vector x, output vector $y = [q\ a_{\text{center}}\ a_{\text{wing,fore}}\ a_{\text{wing,aft}}]^T$, and input vector $u = [\delta_B\ \ \delta_O]^T$. A grid representation with 15 uniformly spaced points is used to cover the domain $V_\infty \in [37.5\ \ 85]$ m/s. The aircraft is naturally stable up to about 70 m/s. Beyond that speed, flutter occurs. Flutter is an unstable oscillation caused by the adverse interaction of aerodynamics and structural dynamics.[6,40,43-46] The purpose of the example controller is to stabilize the aircraft beyond its original flutter speed and provide control of the vertical acceleration a_{center}.

For simplicity, load disturbances are assumed, that is, $\mathbf{P_d} = \mathbf{P_u}$. The weighted mixed sensitivity formulation (38) is set up in the following way. The weighting filter $\mathbf{W_e} = diag\left(1, \frac{0.5\ s+4.33}{s}, 1, 1\right)$ is selected to express the tracking requirement on a_{center} up to a frequency of 5 rad/s and to limit the peak sensitivity in the other channels. The weighting filter $\mathbf{W_u} = diag\left(\frac{0.5\ s+1.73}{s}\frac{100\ s+15\ 000}{s+15\ 000}, \frac{100\ s+15\ 000}{s+15\ 000}\right)$ is selected to restrict the control authority of the body flaps to a frequency range of 2 to 150 rad/s and for the outboard flaps to frequencies below 150 rad/s. The choice $V_e = diag(30, 1, 1, 1)$ reflects a desired maximum pitch rate of 30°/s and maximum wing tip accelerations of 1 g per 1 g vertical acceleration demand. The weight $V_u = 10\,I$ is selected to limit the control surface deflections to 10° per previously specified desired maximum error. Finally, $V_d = 1\,I$ is selected to represent a 10 % uncertainty at the inputs. An observer-based LPV controller is synthesized using steps 2 to 4 of the procedure described in Section 3.3. For comparison, the LPVTools `lpvsyn` routine[8] is used to obtain a controller through conventional output feedback synthesis. (In this case, the integrators in the weighting filters are replaced by $\frac{1}{s+0.0005}$ to satisfy stabilizability requirements.) Both algorithms are configured to result in a 5% suboptimal controller in order to improve numerical behavior.[8,47] They are executed on a Windows 10 64bit standard desktop PC with 3.5 GHz CPU and 8 GB RAM running Matlab 2018b. Both resulting controllers are of order 22.

Figure 7 shows the achieved performance index (upper bound on the induced $\mathcal{L}_2$-norm of the closed loop) and required computational time for increasingly complex basis functions for the Lyapunov matrices $X(p)$,$Y(p)$ and $Y(p)$,$Z(p)$ used in the solution of the SDPs corresponding to Theorem 2 and 5, respectively. For Lyapunov matrices without parameter dependence, the output feedback synthesis takes 29 seconds and results in a clearly better performance index (6.7 vs 12.0) than

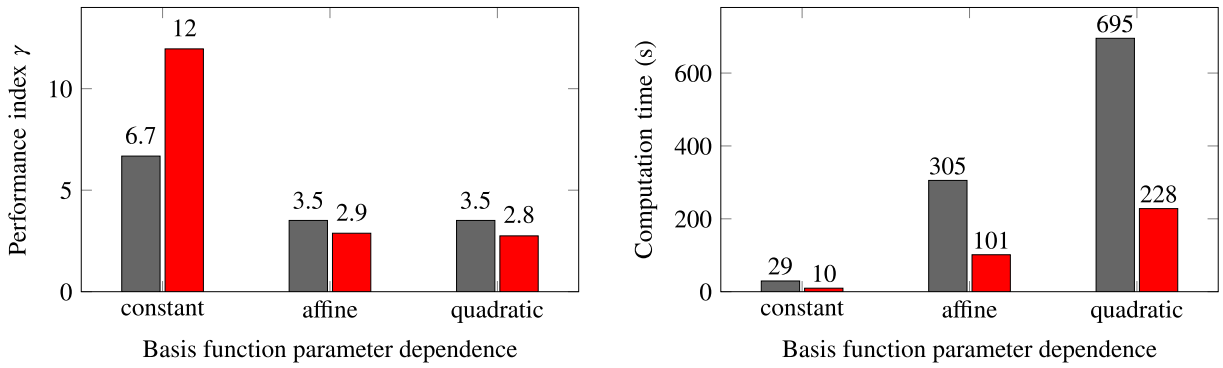

FIGURE 7 Comparison of performance index and computation time (output feedback synthesis ■/observer-based synthesis ■) on a Windows 10 64-bit standard desktop PC with 3.5 GHz CPU and 8 GB RAM running Matlab 2018b [Colour figure can be viewed at wileyonlinelibrary.com]

the observer-based synthesis that takes 10 seconds. The large gap demonstrates the inherent conservatism of the proposed approach. When affinely parameter-dependent matrices, that is, $X(V_\infty) = X_0 + \frac{V_\infty - 37.5}{85-37.5} X_1$, $Y(V_\infty) = Y_0 + \frac{V_\infty - 37.5}{85-37.5} Y_1$ are used, the number of decision variables in the SDP increases. The output feedback synthesis now takes 305 seconds and results in a performance index 3.5. The observer-based synthesis requires 101-second computational time and results in a performance index 2.9. The better performance of the observer-based controller over the output feedback controller might seem surprising. However, it shall be emphasized that specifying the same basis functions for $X(p)$,$Y(p)$ in Theorem 2 and $Y(p)$,$Z(p)$ in Theorem 5 still results in different closed-loop storage functions due to the different meaning of $X(p)$,$Y(p)$ and $Y(p)$,$Z(p)$. Consequently, the observer-based controller might very well outperform the output feedback controller using the same basis functions. It should further be noted that the output feedback controller in this case depends explicitly on the derivative of the scheduling parameter, whereas the observer-based controller only depends on the scheduling parameter. Increasing the basis function complexity to a quadratic function, that is, $X(V_\infty) = X_0 + \frac{V_\infty - 37.5}{85-37.5} X_1 + \left(\frac{V_\infty - 37.5}{85-37.5}\right)^2 X_2$, and $Y(V_\infty)$ analogously further increases the required computational time. The output feedback synthesis now takes 695 seconds but still yields a performance index 3.5, while the observer-based synthesis takes 228 seconds and improves the performance index slightly further to 2.8. In summary, this representative application example shows that the conservatism of the proposed approach can be outweighed by the reduced conservatism associated with using higher order basis functions.

To gain some additional intuition about the sources of conservatism in the proposed approach, the well-understood LTI case is considered as a comparison. In this case, the calculation of $\begin{bmatrix}\mathbf{M} & \mathbf{N_d}\end{bmatrix}$ in accordance with (39) results in a normalized left coprime factorization. A normalized left coprime factorization is coinner, that is, it has the property $\begin{bmatrix}\mathbf{M} & \mathbf{N_d}\end{bmatrix}\begin{bmatrix}\mathbf{M} & \mathbf{N_d}\end{bmatrix}^* = I$, where $*$ denotes the adjoint operator.[10] It follows from this property that all singular values of $\begin{bmatrix}\mathbf{M} & \mathbf{N_d}\end{bmatrix}$ are unity and further that the inequality (31) is, in fact, an equality.[35] Figure 8 shows the optimization objective trace(W) of the SDP (39) for increasingly complex basis functions for $Z(p)$. It further shows the singular values of the resultant parameter-dependent contractive left coprime factorization at fixed parameter values. With increasing complexity of the basis functions, the cost function decreases and the singular values tend to unity, which is the boundary of the feasible set associated with the LMI (39b). As a consequence, the contractive coprime factorization resembles more and more a normalized coprime factorization, pointwise on the parameter domain. A conjecture here is that this minimizes the conservatism associated with inequality (31). The observation also clearly shows the benefit gained by using parameter-dependent basis functions for the coprime factorization in comparison with the approach of Prempain and Postlethwaite.[15]

To finally show that the observer-based synthesis indeed yields a usable controller and that similar performance indices indicate similar control laws, time-domain simulations are compared for the two controllers obtained with quadratic basis functions. Figure 9 shows a step command in vertical acceleration at all 15 design airspeeds. For comparison, a step deflection of the control surfaces of the open-loop system is also shown, which leads to the fast and rapidly increasing unstable oscillation associated with flutter. Both controllers stabilize the system and lead to qualitatively very

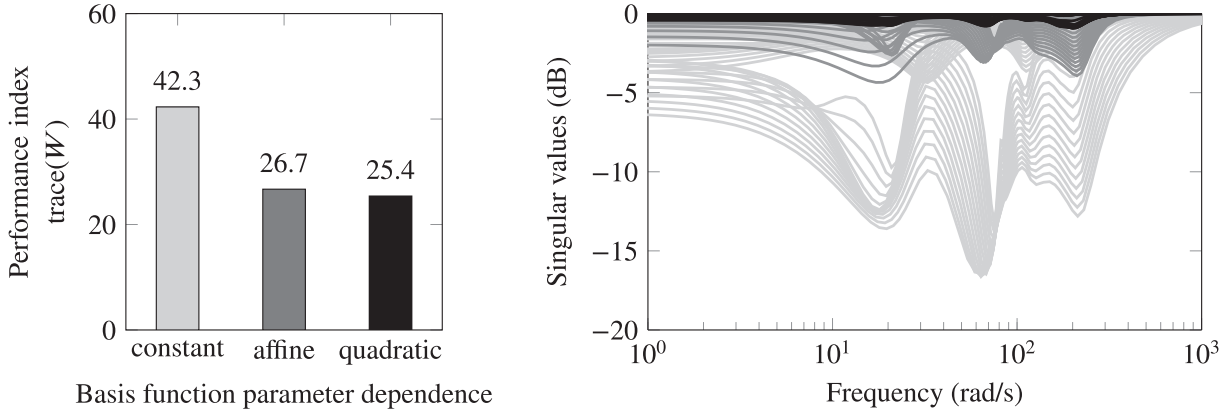

FIGURE 8 Singular values of contractive coprime factorization $[\mathbf{M}\ \mathbf{N_d}]$ with constant (——), affine (——), and quadratic (——) basis function

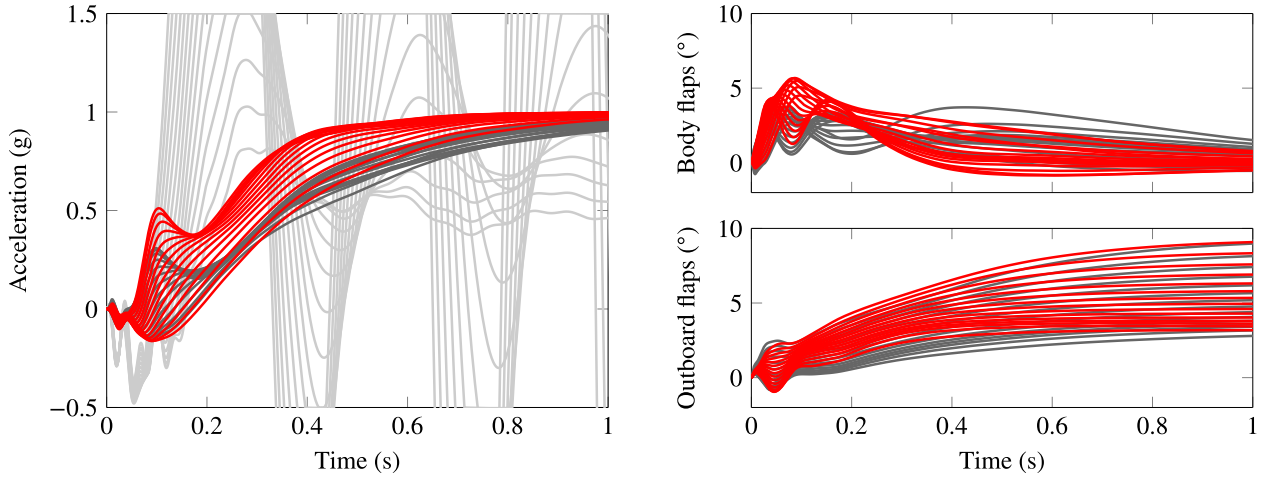

FIGURE 9 Response to 5° flap deflection (open loop ——) and response to 1 g vertical acceleration command (closed loop with output feedback synthesis ——/observer-based synthesis ——) at 15 uniformly spaced airspeeds in [37.5, 85] m/s [Colour figure can be viewed at wileyonlinelibrary.com]

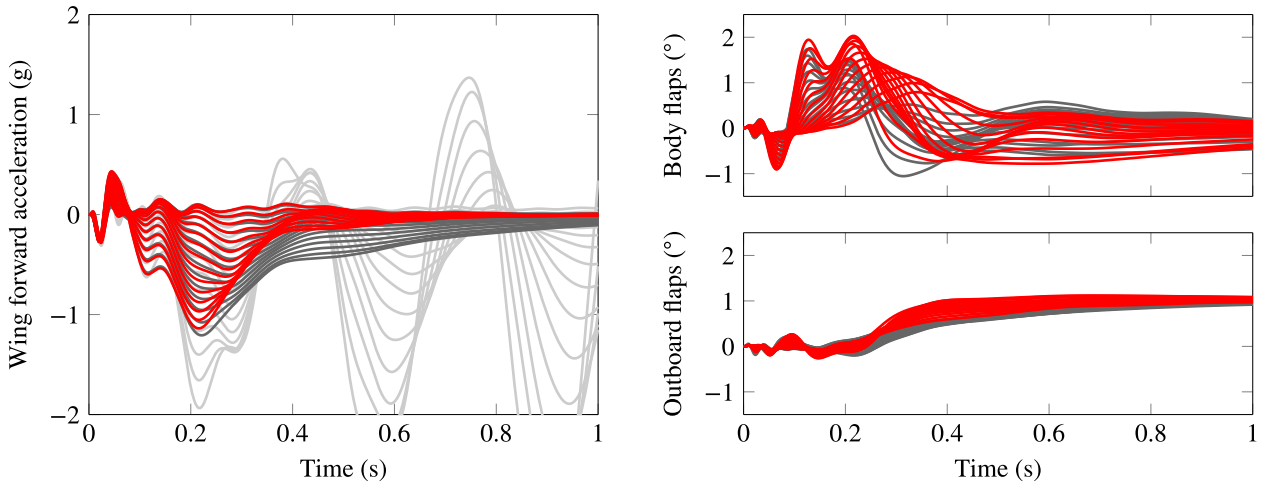

FIGURE 10 Response to a 1° step disturbance at outboard flaps (open loop ——/output feedback synthesis ——/observer-based synthesis ——) at 15 uniformly spaced airspeeds in [37.5, 85] m/s [Colour figure can be viewed at wileyonlinelibrary.com]

similar responses. The observer-based controller is slightly faster, both in terms of rise time and settling time. To achieve this, it uses slightly larger body flap deflections that are, however, still clearly below the specified limits. Figure 10 further shows the fore wing acceleration response to a 1° input disturbance at the outboard flaps. Again, both controllers stabilize the system and improve damping in comparison with the open-loop system. The observer-based controller is again slightly faster than the conventional output feedback controller.

5 | CONCLUSIONS

The proposed two-step observer-based synthesis leads to an output feedback controller with guaranteed closed-loop performance as specified by a weighted mixed sensitivity problem. First, an observer is obtained through calculation of a contractive left coprime factorization of the plant. This observer is shown to maximize the feasible solution set for a subsequent state feedback synthesis such that the achievable performance of the overall procedure is optimized. Compared with the conventional output feedback synthesis, the computation time is significantly reduced and the resulting controller does not explicitly depend on the rate of scheduling parameter variation. The observer-based synthesis, in general,

can be more conservative than directly solving the output feedback problem. However, higher order basis functions for the storage function can be used due to the lower computational complexity, which reduce the conservatism of the design and might even outperform the classical output feedback synthesis. The advantages of this design approach are showcased in a high-fidelity application example, considering active flutter suppression control for an unmanned aircraft.

CONFLICT OF INTEREST

The authors declare no potential conflict of interests.

AUTHOR CONTRIBUTIONS

The authors jointly developed the observer-based controller synthesis method and wrote this article. In detail: conceptualization: J.T. and H.P.; theoretical development and methodology: J.T. and H.P.; software: J.T.; control design for application example: J.T.; original draft preparation: J.T. and H.P.; review and editing: J.T. and H.P.; graphics: J.T.; and supervision: H.P.

ORCID

Julian Theis https://orcid.org/0000-0001-8252-2555
Harald Pfifer https://orcid.org/0000-0001-6734-704X

REFERENCES

1. Becker G, Packard A. Robust performance of linear parametrically varying systems using parametrically-dependent linear feedback. *Syst Control Lett*. 1994;23(3):205-215. https://doi.org/10.1016/0167-6911(94)90006-X.
2. Wu F, Yang XH, Packard A, Becker G. Induced L2-norm control for LPV systems with bounded parameter variation rates. *Int J Robust Nonlinear Control*. 1996;6(9-10):983-998.
3. Apkarian P, Gahinet P, Becker G. Self-scheduled H_∞ control of linear parameter-varying systems: a design example. *Automatica*. 1995;31:1251-1261. https://doi.org/10.1016/0005-1098(95)00038-X.
4. Apkarian P, Gahinet P. A convex characterization of gain-scheduled H_∞ controllers. *IEEE Trans Automat Control*. 1995;40(5):853-864. https://doi.org/10.1109/9.384219.
5. Bennani S, Willemsen D, Scherer C. Robust control of linear parametrically varying systems with bounded rates. *J Guidance Control Dyn*. 1998;21(6):916-922. https://doi.org/10.2514/2.4325.
6. Hjartarson A, Seiler PJ, Balas GJ. LPV aeroservoelastic control using the LPVTools toolbox. Paper presented at: Proceedings of the AIAA Atmospheric Flight Mechanics Conference; 2013. 2013–4742. https://doi.org/10.2514/6.2013-4742.
7. Hjartarson A, Seiler P, Packard A. LPVTools: a toolbox for modeling, analysis, and synthesis of parameter varying control systems. *IFAC-PapersOnLine*. 2015;48(26):139-145. https://doi.org/10.1016/j.ifacol.2015.11.127.
8. Balas GJ, Hjartarson A, Packard A, Seiler PJ. *LPVTools: A Toolbox For Modeling, Analysis, and Synthesis of Parameter Varying Control Systems*. Minneapolis, MN: Software and User's Manual Publisher; 2015.
9. Agulhari CM, Felipe A, Oliveira RCLF, Peres PLD. The robust LMI parser––a toolbox to construct LMI conditions for uncertain systems. *ACM Trans Math Softw*. 2019;45(3):1-25. https://doi.org/10.1145/3323925.
10. Zhou K, Doyle JC, Glover K. *Robust and Optimal Control*. Upper Saddle River, NJ: Prentice Hall. 1st 1996.
11. Wu F. A generalized LPV system analysis and control synthesis framework. *Int J Control*. 2001;74(7):745-759. https://doi.org/10.1080/00207170010031495.
12. Oliveira RCLF, Peres PLD. Parameter-dependent LMIs in robust analysis: characterization of homogeneous polynomially parameter-dependent solutions via LMI relaxations. *IEEE Trans Automat Control*. 2007;52(7):1334-1340. https://doi.org/10.1109/tac.2007.900848.
13. Scherer C. LPV control and full block multipliers. *Automatica*. 2001;37(3):361-375. https://doi.org/10.1016/S0005-1098(00)00176-X.
14. Wu F, Dong K. Gain-scheduling control of LFT systems using parameter-dependent Lyapunov functions. *Automatica*. 2006;42(1):39-50. https://doi.org/10.1016/j.automatica.2005.08.020.
15. Prempain E, Postlethwaite I. L_2 and H_2 performance analysis and gain-scheduling synthesis for parameter-dependent systems. *Automatica*. 2008;44(8):2081-2089. https://doi.org/10.1016/j.automatica.2007.12.008.
16. Apkarian P, Adams RJ. Advanced gain-scheduling techniques for uncertain systems. *IEEE Trans Control Syst Tech*. 1998;6(1):21-32. https://doi.org/10.1109/87.654874.
17. Sato M. Gain-scheduled output-feedback controllers depending solely on scheduling parameters via parameter-dependent Lyapunov functions. *Automatica*. 2011;47(12):2786-2790. https://doi.org/10.1016/j.automatica.2011.09.023.
18. Prempain E. On coprime factors for parameter-dependent systems. Paper presented at: Proceedings of the 45th IEEE Conference on Decision and Control; 2006:5796-5800. https://doi.org/10.1109/CDC.2006.376773
19. Saupe F, Pfifer H. Applied LPV control exploiting the separation principle for the single axis positioning of an industrial manipulator. *IEEE Int Conf Control Appl*. 2011;1476-1481. https://doi.org/10.1109/CCA.2011.6044513.
20. Vidyasagar M. *Control System Synthesis: A Factorization Approach*. 1st ed. Cambridge, MA: The MIT Press; 1985.
21. Sanchez-Peña RS, Sznaier M. *Robust Systems Theory and Applications*. 1st ed. New York, NY: John Wiley & Sons; 1998.

22. Kwakernaak H. Mixed sensitivity design. *IFAC Proc Vol*. 2002;35(1):61-66. https://doi.org/10.3182/20020721-3-US-01236.
23. Kwakernaak H. Mixed sensitivity design: an aerospace case study. *IFAC Proc Vol*. 2002;35(1):49-53. https://doi.org/10.3182/20020721-6-ES-1901.01234.
24. Theis J, Sedlmair N, Thielecke F, Pfifer H. Observer-based LPV control with anti-windup compensation: a flight control example. Paper presented at: Proceedings of the 2020 IFAC World Congress; 2020.
25. Scherer C, Wieland S. Linear matrix inequalities in control. Lecture Notes for a Course of the Dutch Institute of Systems and Control, Delft University of Technology; Delft, Netherlands; 2004.
26. Wu F. *Control of Linear Parameter Varying Systems* (PhD thesis). Berkeley, CA: University of California; 1995.
27. Safonov MG, Limebeer DJN, Chiang RY. Simplifying the $_{H\infty}$ theory via loopshifting, matrix-pencil and descriptor concepts. *Int J Control*. 1989;50(6):2467-2488. https://doi.org/10.1080/00207178908953510.
28. Wood GD. Control of Parameter-Dependent Mechanical Systems (PhD thesis). Cambridge, UK: Cambridge University Press; 1995.
29. Gahinet P, Apkarian P. A linear matrix inequality approach to H_∞ cntrol. *Int J Robust Nonlinear Control*. 1994;4(4):421-448. https://doi.org/10.1002/rnc.4590040403.
30. Lee LH. *Identification and Robust Control of Linear Parameter-Varying Systems* (PhD thesis). Berkeley, CA: University of California; 1997.
31. Nett C, Jacobson C, Balas M. A connection between state-space and doubly coprime fractional representations. *IEEE Trans Automat Control*. 1984;29(9):831-832. https://doi.org/10.1109/TAC.1984.1103674.
32. Meyer DG. Fractional balanced reduction: model reduction via fractional representation. *IEEE Trans Automat Control*. 1990;35(12):1341-1345. https://doi.org/10.1109/9.61011.
33. Glover K, McFarlane D. Robust stabilization of normalized coprime factor plant descriptions with $_{H\infty}$-bounded uncertainty. *IEEE Trans Automat Control*. 1989;34(i):821-830. https://doi.org/10.1109/9.29424.
34. McFarlane DC, Glover K. *Robust Controller Design Using Normalized Coprime Factor Plant Descriptions*. 1st ed. New York, NY: Springer; 1990.
35. McFarlane DC, Glover K. A loop-shaping design procedure using $_{H\infty}$ synthesis. *IEEE Trans Automat Control*. 1992;37(6):759-769. https://doi.org/10.1109/9.256330.
36. Balas G, Chiang R, Packard A, Safonov M. *Robust Control Toolbox R2018b. Reference*. Natick, MA: The MathWorks; 2018.
37. Doyle JC, Glover K, Khargonekar PP, Francis BA. State-space solutions to standard H_2 and H_∞ control problems. *IEEE Trans Automat Control*. 1989;34(8):831-847. https://doi.org/10.1109/9.29425.
38. Zhou K, Khargonekar PP. An algebraic Riccati equation approach to H_∞ optimization. *Syst Control Lett*. 1988;11:85-91. https://doi.org/10.1016/0167-6911(88)90080-1.
39. Theis J. *Robust and linear parameter-varying control of aeroservoelastic systems* (PhD thesis). Hamburg, Germany: Hamburg University of Technology; 2018
40. Theis J, Pfifer H, Seiler P. Robust modal damping control for active flutter suppression. *J Guidance Control Dyn*. 2020;43(6):1056-1068. https://doi.org/10.2514/1.G004846.
41. Ryan JJ, Bosworth JT, Burken JJ, Suh PM. Current and future research in active control of lightweight, flexible structures using the X-56 aircraft. Paper presented at: Proceedings of the 52nd AIAA Aerospace Sciences Meeting; 2014:Paper No. 0597. https://doi.org/10.2514/6.2014-0597
42. Schulze PC, Danowsky B, Lieu T. High fidelity aeroservoelastic model reduction methods. Paper presented at: Proceedings of the AIAA Atmospheric Flight Mechanics Conference; 2016:Paper No. 2016-2007. https://doi.org/10.2515/6.2016-2007
43. Livne E. Aircraft active flutter suppression: state of the art and technology maturation needs. *J Aircraft*. 2018;55(1):410-452. https://doi.org/10.2514/1.c034442.
44. Roger KL, Hodges GE, Felt L. Active flutter suppression—a flight test demonstration. *J Aircraft*. 1975;12(6):551-556. https://doi.org/10.2514/3.59833.
45. Theis J, Pfifer H, Seiler P. Robust control design for active flutter suppression. Paper presented at: Proceedings of the AIAA Atmospheric Flight Mechanics Conference; 2016:Paper No. 2016-1751. https://doi.org/10.2514/6.2016-1751
46. Pusch M, Ossmann D, Luspay T. Structured control design for a highly flexible flutter demonstrator. *Aerospace*. 2019;6(3):27. https://doi.org/10.3390/aerospace6030027.
47. Saupe F. *Linear Parameter Varying Control Design for Industrial Manipulators* (PhD thesis). Hamburg, Germany: Hamburg University of Technology; 2013.

How to cite this article: Theis J, Pfifer H. Observer-based synthesis of linear parameter-varying mixed sensitivity controllers. *Int J Robust Nonlinear Control*. 2020;30:5021–5039. https://doi.org/10.1002/rnc.5038